Enzymatic Synthesis and Solid-State Properties of Aliphatic Polyesteramides with Polydimethylsiloxane Blocks

Bhaskar Sharma, Abul Azim, Himanshu Azim, and Richard A. Gross*

NSF−I/UCRC Center for Biocatalysis and Bioprocessing of Macromolecules, Polytechnic University, Department of Chemistry and Chemical Engineering, Six Metrotech Center, Brooklyn, New York 11201

Elisa Zini, Maria Letizia Focarete, and Mariastella Scandola*

University of Bologna, Department of Chemistry "G. Ciamician" and National Consortium of Materials Science and Technology (INSTM, UdR Bologna), via Selmi 2, 40126 Bologna, Italy

Received March 20, 2007; Revised Manuscript Received August 14, 2007

ABSTRACT: The synthesis of silicone polyesteramides was successfully performed in bulk at 70 °C via a biocatalytic route. Immobilized *Candida antartica* Lipase B (Novozym 435, N435) was used as catalyst under mild conditions to perform the polycondensation reaction using various feed mole ratios of diethyl adipate (DEA), 1,8-octanediol (OD), and α,ω-(diaminopropyl)polydimethylsiloxane (Si-NH_2). The syntheses of poly(octamethylene adipate), POA, and poly(α,ω-(diaminopropyl)polydimethylsiloxane adipamide), PSiAA, were also performed by N435 catalysis in order to compare their properties with those of silicone polyesteramides. The microstructures of all polymers were studied by ^{1}H NMR spectroscopy, and calculated amide/ester ratios were in agreement with the monomer feed mole ratio. Formation of amide links (DEA−SiAA units) occurs more rapidly than ester repeats (DEA−OA units). This results in copolymers that tend toward a blocklike sequence distribution. Thermal stability of the polyesteramides, evaluated by TGA both in nitrogen and in air, increases with DEA−SiAA content (up to 50 mol %). The relative amount of amide and ester units along the polymer chain strongly affects the physical aspect of the polyesteramides. High content of DEA−OA units leads to hard solid materials containing a well-developed high melting POA-type crystal phase, whose melting temperature changes with composition. When DEA−SiAA units are the major component, the material acquires a sticky appearance.

Introduction

Silicone-based polymers can be used in numerous applications due to their versatile and unique properties. The large bond angle (ca. 145°) and low bending force constant of Si−O−Si linkages endow silicones with high chain flexibility.[1] Moreover, the Si−O bond is characterized by high bond energy (106 kcal/mol).[2] As a consequence, silicones are thermally stable over a wide temperature range and can replace organic materials that would melt or decompose at high temperatures. Indeed, degradation of dimethylsilicone fluids begins at 350 °C.[3] Furthermore, these polymers possess a very low glass transition temperature, typically less than −120 °C, which reflects the ease of segmental motions along the chain.[4] They also have flame-retardant properties, are resistant to UV radiation and to ozone, and exhibit low chemical reactivity, high gas permeability, and physiological inertness.[5] The exceptional hydrophobicity of silicones along with their fluid nature allows them to wet out or spread over surfaces.[6] Among polysiloxanes, polydimethylsiloxane (PDMS) is one of the most widely investigated materials that is also recognized for its biocompatibility.[7] Methyl groups of PDMS form a hydrophobic sheath around the polar siloxane backbone, resulting in reductions in both surface energy and surface tension. As a consequence, this polymer has a strong nonpolar character, and its solubility parameter is much lower than other common polymers. This peculiarity is responsible for the well-known thermodynamic incompatibility of PDMS with most polymers.[5]

PDMS converted into reactive intermediates by introduction of functional groups at chain ends enables their incorporation as block units in copolymers. A number of polymers containing siloxane units are reported in the literature. Haupt et al.[8] described the synthesis of water-soluble PDMS with pendant sugar moieties for potential biomedical applications. These polymers have both a hydrophobic backbone, providing chemical and biological stability, and natural hydrophilic saccharide side-chain residues (glycopolymers) that enable tailoring of amphiphilic character and bioactivity.[9,10] Polymers with recurring siloxane moieties and other heat-resistant groups such as amides are also known in the literature.[11−13] Sacripante and Macaneny[14] disclosed that polyesteramides containing siloxane segments are useful in toner and developer formulations. In addition, PDMS copolymers have been designed for use as surface modifiers.[7,15,16] By changing siloxane block length and content, and by using an appropriate comonomer, PDMS copolymers can be tailored for specific applications. By blending PDMS block copolymers with other polymeric components, siloxane segments migrate to the air−polymer interface, thereby enriching the material surface in the silicone component.[7] The resulting surfaces of such materials take on silicone-like properties (hydrophobic, biocompatible, flame retardant) while polymer bulk properties remain unaffected.[7] For example, a small amount of PDMS−polycaprolactone block copolymer in blends with PVC was used to improve the materials blood compatibility.[7]

Generally, siloxane-based copolymers are synthesized by chemical methods, under harsh conditions,[17] that results in uncontrolled redistribution and side reactions.[18] High polymerization temperatures and acid/base catalysts cause decomposition of useful functional groups in siloxane monomer or macromer building blocks such as alkene and epoxy moieties. For example, silicone-containing polyester polyols are of interest

* To whom correspondence should be addressed.

10.1021/ma070671i CCC: $37.00
Published on Web 10/03/2007

Scheme 1. N435-Catalyzed Polymerization of α,ω-(Diaminopropyl)polydimethylsiloxanes, Diethyl Adipate, and 1,8-Octanediol at 70 °C in Bulk

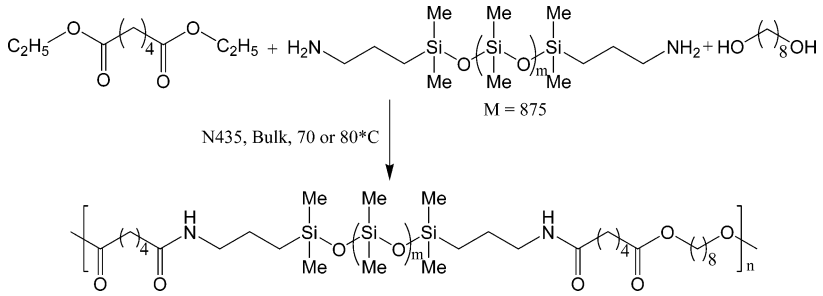

as macromers for incorporation into polyurethanes to modify their surface properties.[19] To prepare silicone-modified polyester polyols, diacids, diols, and hydroxyl-terminated PDMS with 1 wt % titanium catalyst were reacted at 140−180 °C for 12−16 h. Also, water-soluble PEG−silicone polyesters surfactants were prepared by polymerization of poly(ethylene glycol) (PEG), maleic anhydride (MA), polydimethylsiloxane, and fumaric acid using titanium isopropoxide as catalyst at 180 °C under a nitrogen atmosphere and then maintained at this temperature for 8 h. In the second step, 2 mol of PEG and 1 mol of polydimethylsiloxane were reacted in the presence of the same catalyst at 180 °C for ∼16 h.[20]

Polyamides are generally prepared by mixing equimolar amounts of dibasic acids and diamines at polymerization temperatures between 260 and 280 °C.[21] While high reaction rates and conversions may be achieved through acid or base catalysis, these catalysts may induce the decomposition of potentially useful functional groups as discussed above. Coupling reagents, such as dicylohexylcarbodiimide, that function under mild reaction conditions in organic media can preserve sensitive moieties such as silicones and vinyl groups. However, they are inefficient since they require one molecule of coupling agent per bond forming step. Furthermore, coupling agents and acid/base catalysts are not regioselective. An example of polycondensation reactions between *O*-acetylgalactaric acid chlorides and PDMS diamines was recently reported to give high molecular weight polyamides (M_w = 103 600 g/mol).[22] 2,3,4,5-Tetra-*O*-acetylgalactaroyl dichloride was reacted for 5 days with a PDMS diamine in chloroform solution with triethylamine at 0 °C. Disadvantages of this method include (i) use of a protected sugar due to the nonselectivity of the reaction, (ii) need to activate the diacid by formation of an acid chloride, and (iii) liberation of stoichiometric quantities of an organic salt byproduct.

In contrast, enzymatic catalysis can proceed with high enantio- and regioselectivity under mild conditions, providing an attractive alternative to conventional chemical methods for the preparation of a wide range of small molecules, macromers, and polymers. Recently, a review was published documenting research on enzymatic polyester synthesis by polycondensation reactions.[23] Since then, our laboratories reported effects of alditol structure on polyol−polyester synthesis[24] as well as that cutinases are active catalysts for polyester synthesis.[25] Tanaka et al.[26] and Uejima et al.[27] described the preparation of low molar mass organosilicon esters by lipase catalysis under mild conditions. Furthermore, "sweet silicone" bolamphiphiles were prepared in our laboratory catalyzed by immobilized Lipase B from *Candida antarctica* (Novozym 435, N435). N435 catalysis resulted in regioselective (at position C6) formation of ester bonds between carboxylic acid end-functionalized organosilicones and α,β-ethyl glucoside.[28] Lipase-catalyzed aminolysis of carboxylic esters have become common methods for the preparation of amides.[29] Synthesis of oleamide, used in plastics processing as slip and antiblocking agents, is normally performed by enzymatic ammonolysis of triolein with ammonia catalyzed by N435.[30] Dow Corning and our laboratory disclosed for the first time polymers consisting of organosilicone esters or amides prepared by enzyme catalysis.[31] In one example, a reaction between dimethyl adipate and a diamine disiloxane, performed in bulk at 70 °C for 12 h and catalyzed by N435, resulted in an organosilicone polyamide with M_n = 2100.

The present paper describes a one-pot synthesis of silicone polyesteramides by lipase catalysis. Lipase B from *Candida Antartica*, CALB, physically immobilized on Lewatit (N435), was used to catalyze reactions between diethyl adipate (DEA), 1,8-octanediol (OD), and α,ω-(diaminopropyl)polydimethylsiloxane ($SiNH_2$) under mild conditions. To the best of our knowledge, this is the first report after the initial disclosure in ref 31 that describes a biocatalytic route to aliphatic polyesteramides containing siloxane units. To characterize physical properties of synthesized products, solid-state analyses were performed by thermogravimetric analysis (TGA), wide-angle X-ray scattering (WAXS), and differential scanning calorimetry (DSC).

Experimental Section

Materials. All chemicals were of analytical grade and were used as received. Novozym 435 (N435, specific activity 10 000 PLU/g) was a gift from Novozymes (Bagsvaerd, Denmark). N435 consists of Lipase B from Candida Antartica (CALB) physically immobilized on acrylic macroporous beads. α,ω-(Diaminopropyl)-polydimethylsiloxane (M_w = 875, M_w/M_n = 1.30) was supplied by Gelest, Inc. (Tullytown, PA). 1,8-Octanediol, diethyl adipate, and deuterated chloroform were purchased from Aldrich Co. Chloroform and tetrahydrofuran were purchased from Pharmaco. All solvents were of HPLC grade. If not otherwise specified, chemicals above were purchased in the highest available purity and used as received (without further purification).

Synthetic Methods. *General Method for Polymerization Reactions.* Novozym 435 (10 wt % relative to total monomer, i.e., 1 wt % protein relative to total monomer), dried in a vacuum (1 mmHg, 25 °C, 24 h), was transferred into a 100 mL round-bottom flask containing diethyl adipate (2.02 g, 10 mmol) and a mixture (10 mmol total) of 1,8 octanediol and α,ω-(diaminopropyl)polydimethylsiloxane in different ratios (Scheme 1). Reactions were performed in bulk at 70 °C for up to 70 h. The flask was capped with an adaptor connected to a vacuum manifold and then placed into an oil bath maintained at 70 °C under ambient pressure. After 40 h, the reaction mixture was placed under reduced pressure (10−20 mmHg) for the remaining reaction period. The reaction was terminated by adding an excess of chloroform to the crude product, stirring for 15−20 min, removing Novozym 435 by filtration, and stripping the chloroform by rotoevaporation.

Instrumental Methods. Proton nuclear magnetic resonance (^{1}H NMR) spectra were recorded on a Bruker NMR spectrometer (model DPX300) at 300 MHz in deuterated chloroform as solvent.

Table 1. Synthesis of Silicon Polyamide by Reaction of 875 α,ω-(Diaminopropyl)polydimethylsiloxane with Diethyl Adipate, Catalyzed by N435 at 70 and 80 °C

sample no.	time (h)	M_n,[a] 70 °C	M_w/M_n,[a] 70 °C	M_n,[a] 80 °C	M_w/M_n,[a] 80 °C
1	0.5	775	2.2	690	2.3
2	1	980	2.2	920	2.2
3	2	3700	2.0	3800	2.1
4	8	4900	1.9	5100	2.0
5	10	5100	1.8	5500	1.7
6	24	6300	1.6	7000	1.5

[a] From GPC.

^{1}H NMR chemical shifts in parts per million (ppm) were referenced relative to chloroform ($\delta = 7.26$ ppm) as an internal standard. The number- and weight-average molecular weights (M_n and M_w, respectively) were determined by gel permeation chromatography (GPC). GPC measurements were performed on a Waters HPLC system (Waters Corp., Milford, MA) equipped with a 510 pump, a model 717 plus injector, and a model 410 differential refractometer. A column set used for chromatography consists of Polymer Laboratories PL 10^4 Å and 500 Å columns in series. Tetrahydrofuran (HPLC grade) was used as the mobile phase at flow rate of 1.0 mL/min. Calibration was accomplished using polystyrene standards (from Polymer Laboratories Ltd.). Thermogravimetric analysis (TGA) was performed either in nitrogen or in air atmosphere by means of a TA Instruments TGA2950 thermogravimetric analyzer. The measurements were carried out using a heating rate of 10 °C/min in the temperature range from room temperature to 600 °C. Differential scanning calorimetry (DSC) was performed using a TA Instruments Q100 DSC equipped with the LNCS low-temperature accessory. The temperature scale was calibrated with high-purity standards, and DSC scans were run in the temperature range from −170 to 120 °C in a helium atmosphere at 20 °C/min. Controlled cooling at 10 °C/min or quench cooling was applied between heating runs. Wide-angle X-ray diffraction measurements (WAXS) were carried out at room temperature with a PANalytical X'Pert PRO diffractometer equipped with an X'Celerator detector (which allows ultrafast data collection). Cu anode was used as X-ray source (K radiation: $\lambda = 0.154$ 18 nm, 40 kV, 40 mA), and a 1/4° divergence slit was used to collect the data in the 2θ range from 2° to 60°. The degree of crystallinity (χ_c) was evaluated from diffractograms as the ratio of crystalline peak area to the total area under the scattering curve. After subtracting the contribution of the empty sample holder, the amorphous and crystalline contributions were calculated using the WinFit program by a fitting method.

Results and Discussion

The synthesis of silicone polyamides was investigated in bulk by one-pot enzyme-catalyzed polycondensation reactions between equimolar quantities of diethyl adipate (DEA) and α,ω-(diaminopropyl)polydimethylsiloxane ($SiNH_2$, $M_w = 875$ and $M_w/M_n = 1.30$) (Scheme 1 and Table 1). The enzyme-catalyst system, Novozym 435 (N435), consists of 10 wt % *Candida antartica* Lipase B (CALB) physically immobilized on the macroporous support Lewatit (see above). Reactions formed monophasic mixtures at 70 °C, obviating the need for a solvent. The content of CALB relative to total reactants was 1 wt %.

Previous work by us and others established that N435-catalyzed polycondensation reactions are preferably conducted at between 70 and 90 °C.[24,32] With this knowledge, and taking into account concerns over redistribution reactions,[18] studies to establish preferred reaction temperature and time were performed at 70 and 80 °C. Results of experiments performed for reaction times up to 24 h with values of molecular weight averages for nonfractionated products are compiled in Table 1. Visual inspection showed that, as reactions progressed, magnetic stirring slowed substantially and reaction viscosity continually increased. On the basis of results of molecular weight vs reaction time, Table 1 shows that reactions progressed similarly as a function of reaction time at both 70 and 80 °C. For example, after 8 h at 70 and 80 °C, values of product molecular weight and polydispersity were very close to each other ($M_n = 4900$, $M_w/M_n = 1.9$ at 70 °C, $M_n = 5100$, $M_w/M_n = 2.0$ at 80 °C). Similarly, after 24 h, M_n values of silicone polyamides at 70 and 80 °C were 6300 and 7000, respectively. Polydispersity of silicone polyamides at 70 °C decreased from 2.2 to 1.9 and 1.6 at 0.5, 8, and 24 h, respectively (Table 1). From these results, we cannot conclude that N435-catalyzed polyesteramide synthesis occurs with "chain selectivity", as was previously observed for N435-catalyzed polycondensations to prepare polyesters.[24] Control reactions performed exactly as above at 80 °C but without addition of N435 gave a mixture of monomers and dimers. Hence, results in Table 1 validate that N435 functions as a mild catalyst for condensation polymerizations between PDMS diamines and diesters. Since there was little difference in the course of product formation as a function of reaction time at 70 and 80 °C, and given our preference to work at low temperatures with silicone substrates, 70 °C was selected for further studies on terpolymerizations described below.

Silicone polyesteramides were synthesized in bulk catalyzed by N435. Reactions were performed at 70 °C, for 68−70 h, by one-pot enzyme-catalyzed polycondensation reactions between DEA, 1,8-octanediol (OD) and $SiNH_2$ (Scheme 1 and Table 2). As above, all reactant compositions formed monophasic mixtures at 70 °C, avoiding the need to use a solvent. Poly(octamethylene adipate), POA, and poly(α,ω-(diaminopropyl)-polydimethylsiloxane adipamide), PSiAA, were synthesized by identical reaction conditions. Assignment of signals in NMR spectra of POA and PSiAA enabled interpretation of polyesteramide spectra, providing information on repeat unit compositions and microstructures (see below). Furthermore, POA polyester and PSiAA polyamide were used as reference polymers for comparison of thermal and physical properties of newly synthesized polyesteramides.

Table 2. Silicone Polyesteramide Copolymers and Reference Homopolymers: Poly(octamethylene adipate) (POA) and Poly(α,ω-dipropylpolydimethylsiloxane adipamide) (PSiAA)

sample	feed ratio (mol %) DEA:OD:$SiNH_2$	M_n[a]	M_w/M_n[a]	amide/ester ratio[b]	A:B[c] molar ratio	physical aspect
POA	1:1:0	14000	2.1	0:1	0:100	solid
P(OA-*co*-2 mol % SiAA)	1:0.98:0.02	10100	2.2	1:59	2:98	solid
P(OA-*co*-5 mol % SiAA)	1:0.95:0.05	7200	1.8	1:17.4	5:95	solid
P(OA-*co*-10 mol % SiAA)	1:0.9:0.1	10700	2.3	1:9	10:90	waxy
P(OA-*co*-16 mol % SiAA)	1:0.84:0.16	6700	1.8	1:5.1	16:84	waxy
P(OA-*co*-33 mol % SiAA)	1:0.67:0.33	2800	1.7	1:2	33:67	sticky
P(OA-*co*-50 mol % SiAA)	1:0.5:0.5	11000	1.6	1:1	50:50	sticky
P(OA-*co*-80 mol % SiAA)	1:0.2:0.8	6300	1.5	4:1	80:20	sticky
PSiAA	1:0:1	9400	1.6	1:0	100:0	sticky

[a] From GPC. [b] From ^{1}H NMR: the ratio of integration values of $\mathbf{CH_2}$NHCO/$\mathbf{CH_2}$OCOO. [c] A- and B-units are defined in Scheme 2. The calculation is as follows: A = (mol amide)/(mol ester + mol amide) × 100 and B = (100 − A).

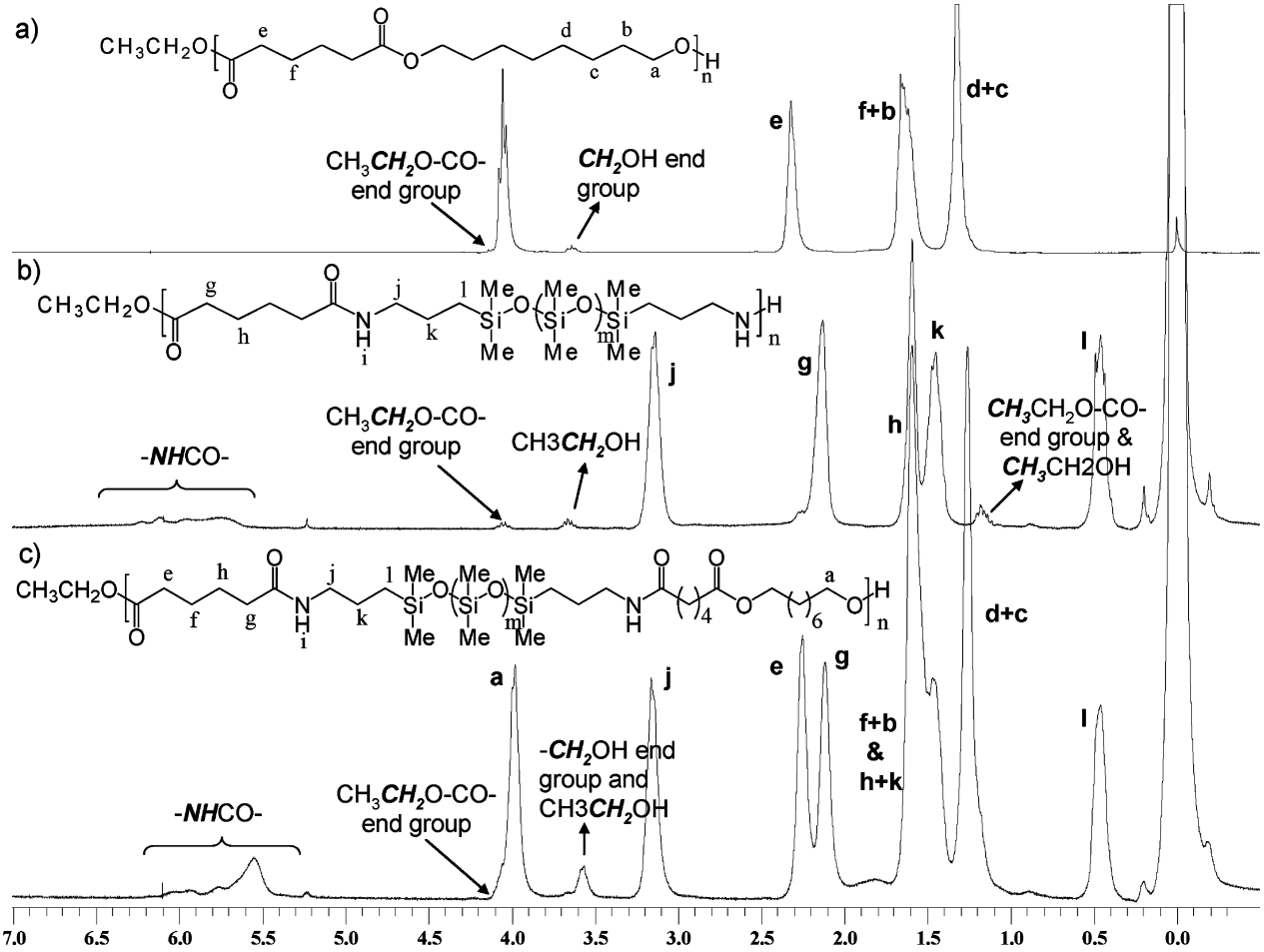

Figure 1. ^{1}H NMR spectra of (a) poly(octamethylene adipate), POA, (b) poly(α,ω-(diaminopropyl)polydimethylsiloxane adipamide), PSiAA, and (c) P(OA-*co*-50 mol % SiAA).

Structural Characterization. ^{1}H NMR spectroscopy reveals the microstructure of polymers synthesized by reacting DEA with an equimolar amount of OD plus $SiNH_2$ where the ratio of OD to $SiNH_2$ is varied. ^{1}H NMR spectra of DEA/OD/$SiNH_2$ polymers with feed ratios of 100/100/0, 100/0/100, 100/50/50 are shown in parts a, b, and c of Figure 1, respectively. The spectrum of POA (Figure 1a) and corresponding assignments below are consistent with those previously reported.[32] High-intensity signals for methylene protons at 4.05 and 2.32 ppm are due to OD unit CH_2O-CO (**a**) and adipate unit CH_2CO-O (**e**) protons, respectively. The low-intensity signal at 4.10 ppm, corresponding to CH_3CH_2O-CO (ester) end groups, is a shoulder on the downfield side of OD (**a**) protons. Methylene CH_2OH end-group protons are well resolved at 3.65 ppm. Assignments of remaining methylene protons, belonging to adipate and OD repeat units, are given in Figure 1a.

In the ^{1}H NMR spectrum of PSiAA (Figure 1b), CH_2NH-CO protons of amide groups are found at $\delta = 5.5-6.3$ ppm. All silicone segment methyl protons, $Si(CH_3)_2-O$, appear together at 0.0 ppm. Chemical shifts corresponding to methylene protons of CH_2NH-CO (**j**) and CH_2CO-NH (**g**) moieties are at 3.13 and 2.12 ppm, respectively, confirming the occurrence of polyamidation reactions between DEA and $SiNH_2$. While low-intensity ester end-group methylene protons (CH_3CH_2O-CO) at 4.05 are overlapped with CH_2O-CO (**a**) protons in Figure 1a, they are well-resolved in Figure 1b. Other signals at 1.60, 1.45, and 0.45 ppm are due to methylene protons CH_2-CH_2CO (**h**), CH_2CH_2NH (**k**), and CH_2Si (**l**), respectively. The presence of residual ethanol in products was confirmed by signals at 3.65 and 1.18 ppm corresponding to ethanol CH_3CH_2-OH and CH_3CH_2OH protons, respectively.

The ^{1}H NMR spectrum of P(OA-*co*-50 mol % SiAA) is displayed in Figure 1c. Signals at 5.5−6.3 and 4.05 ppm correspond to protons of amide (CO*NH*) and ester (CH_2O-CO) groups consistent with formation of copolymers with both amide and ester links. All peak assignments in Figure 1c are consistent with those above and represent a juxtaposition of signals corresponding to DEA−OA (Figure 1a) and DEA−SiAA (Figure 1b) units.

Table 2 displays ratios of amide to ester links determined from spectral integration of signals corresponding to methylene protons CH_2NH-CO (**j**) and CH_2O-CO (**e**). ^{1}H NMR analysis reveals that the ratios of amide/ester links in all copolymers are in agreement with the monomer feed ratios used. Silicone polyesteramide copolymers can be ideally considered as composed of two units whose chemical structure is schematically drawn in Scheme 2, i.e., an amide unit containing the silicone block (A-unit) and an ester unit (B-unit). The A:B molar ratio of all copolymers is reported in Table 2.

Table 2 also has M_n and M_w/M_n values of synthesized nonfractionated polymers determined by GPC in THF. POA, synthesized using an equimolar ratio of DEA to OD, has the highest molecular weight ($M_n = 14\,000$). PSiAA and all copolymers have M_n and PDI values that fall within the range of 6−11 kDa and 1.5−2.2, respectively, except for P(OA-*co*-33 mol % SiAA) whose M_n is lower (2800 Da). Thus, N435 catalysis was successful in synthesizing a wide range of copolymers containing variable ratios of silicone (DEA−SiAA,

Scheme 2. Chemical Structure of Poly(α,ω-dipropylpolydimethylsiloxane adipamide), PSiAA (A-Unit), and Poly(octamethylene Adipate), POA (B-Unit) (See Text)

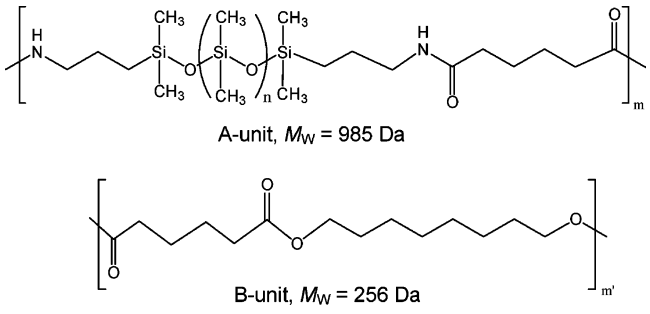

A-unit) and ester (DEA−OA, B-unit) dyads, under mild reaction conditions, without resorting to undesirable chemical approaches described in the Introduction section.

Further Investigations of N435-Catalyzed Synthesis of Polyesteramides. Studies were performed to better understand the relative rates of amide and ester group formation for the above terpolymerizations. First, comparison between copolymerizations of DEA with $SiNH_2$ to prepare PSiAA, and DEA with OD to give POA, were performed under identical conditions described above for polyesteramide terpolymerizations. That is, reactions were conducted at 70 °C, in bulk, at ambient pressure for the first 40 h and, thereafter, at reduced pressure (10−20 mmHg). Consumption of functional groups (p) was monitored at preselected reaction times by analyzing ^{1}H NMR spectra that distinguish signals corresponding to end groups and formation of DEA−SiAA and DEA−OA repeat units (see above). From the Carothers equation (see Table 3, footnote *b*), values of average degree of polymerization (P_n) were determined. GPC values of molecular weight averages were also measured. Results of both DEA/$SiNH_2$ and DEA/OD copolymerizations are listed in Table 3, and functional group conversion (p) values are plotted in Figure 2. Conversion of amine ($-CH_2NH_2$) to amide (CONH−) moieties increased continuously with increased reaction time, reaching 97% corresponding to $P_n = 27$ in 68 h (Figure 2 and Table 3). The polydispersity narrowed with increasing reaction time, most likely due to more rapid consumption of the low molecular weight oligomer population due to its relatively higher diffusivity in the reaction medium. For DEA/OD copolymerizations, initial conversion of hydroxyl ($-CH_2OH$) to ester (CH_2OCOO-) groups was rapid, reaching 89% by 0.25 h. In comparison, conversion of amine to amide moieties occurred slowly, reaching 54% by 0.25 h. However, functional group conversion for POA synthesis

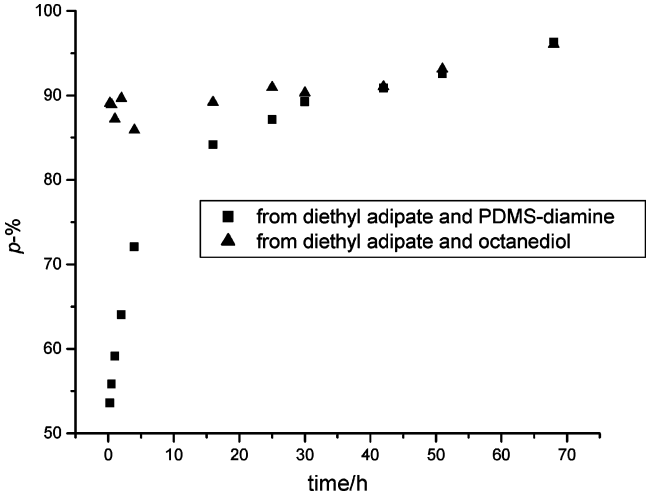

Figure 2. Consumption (p) of amine and hydroxyl functionality as a function of time for N435-catalyzed diethyl adipate/octanediol and diethyl adipate/PDMS-diamine copolymerizations. Reactions were conducted at 70 °C, in bulk, at ambient pressure for the first 40 h and, thereafter, at reduced pressure (10−20 mmHg).

remained almost unchanged from 0.25 h to about 42 h and, thereafter, when vacuum was applied, p values increased slowly, reaching 96.1% in 68 h. In contrast, conversion to amide units continued slowly from 0.25 to 68 h reaching 96.3%. Ultimately, functional group conversion values for both POA and PSiAA were nearly identical at 42, 51, and 68 h. Corresponding values of P_n and M_n for the above reaction times and functional conversions are listed in Table 3. The origin of this difference between ester and amide group functional conversion can be explained as follows. During N435-catalyzed synthesis of POA and PSiAA, ester formation occurs more rapidly than amide formation, resulting in more rapid chain growth over the first 0.25 h. However, ethanol formed as a byproduct during POA synthesis remains in reactions during the first 40 h, since reactions were conducted at ambient pressure. The presence of ethanol in the reaction mixture results in concurrent chain growth by ester formation and depolymerization by transesterification reactions with ethanol. After applying vacuum removing ethanol from reactions, the degree of polymerization increases from 11.1 to 25.6 at 42 and 68 h, respectively (Table 3). In contrast, it appears that the equilibrium during PSiAA synthesis lies toward amide formation so that the reverse reaction resulting in PSiAA chain cleavage is much slower than corresponding reactions between ethanol and POA. Therefore, growth of PSiAA chains occurs continuously throughout polymerizations. Nevertheless, application of vacuum during PSiAA synthesis results in a large

Table 3. N435-Catalyzed Diethyl Adipate/Octanediol and Diethyl Adipate/PDMS-Diamine Copolymerizations[a]

	polycondensation: diethyl adipate and PDMS-diamine				polycondensation: diethyl adipate and octanediol			
time/h	P_n[b]	M_n (NMR)[c]	M_n[d]	PDI[d]	P_n[b]	M_n (NMR)[c]	M_n[d]	PDI[d]
0.25	2.2	1110	390	2.9	9.1	1210	1970	1.4
0.50	2.3	1160	390	2.8	9.1	1210	2480	1.4
1	2.4	1250	430	2.7	7.8	1050	1860	1.3
2	2.8	1410	450	2.7	9.6	1280	2280	1.4
4	3.6	1810	520	2.6	7.1	950	1760	1.3
16	6.3	3160	1260	2.3	9.3	1230	2390	1.4
25	7.8	3890	1685	2.1	11.1	1470	2490	1.4
30	9.3	4650	1960	2.0	10.3	1370	2610	1.4
42	11.1	5520	2940	1.9	11.1	1470	2680	1.4
51	13.5	6700	4070	1.8	14.5	1900	3610	1.5
68	27.0	13360	6860	1.7	25.6	3350	6790	1.7

[a] Reactions were conducted at 70 °C, in bulk, at ambient pressure for the first 40 h and, thereafter, at reduced pressure (10−20 mmHg). [b] By Carother's equation: $P_n = 1/(1 - p)$, where p is the consumption of functionality or extent of the reaction. [c] M_n(NMR) = P_n × [(molecular weight of the repeat unit)/(number of monomers units in the repeat unit)] + molecular weight of end group. [d] From GPC.

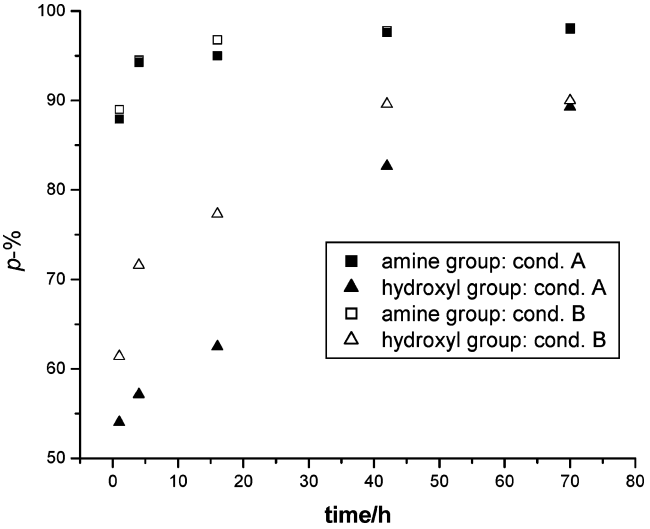

Figure 3. Consumption (p) of amine and hydroxyl function groups vs time for N435-catalyzed terpolymerizations (70 °C, in bulk) between diethyl adipate, octanediol, and PDMS-diamine using a monomer feed of 100:50:50. Reaction conditions were as follows: (i) condition A, no vacuum was applied until 40 h; (ii) condition B, apply a vacuum at 1 h of 100 mmHg that was decreased stepwise to 25 and 2 mmHg by reaction times of 23 and 46 h, respectively.

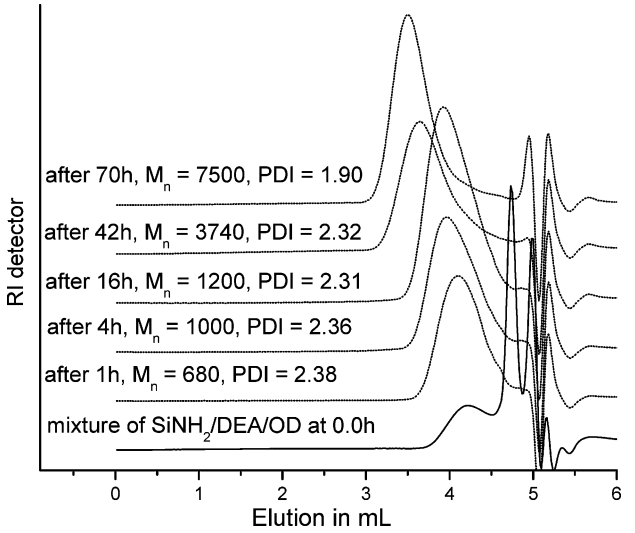

Figure 4. GPC chromatograms for terpolymerizations described in Table 4 performed using condition A.

increase in the degree of polymerization, from 11.1 to 27.0 at 42 and 68 h, respectively. Thus, the presence of ethanol during PSiAA synthesis is either resulting in exchange reactions or, more likely, ethanol inhibits CALB activity.

The concepts developed during the above comparison of PSiAA and POA synthesis were further evaluated for terpolymerization reactions between DEA, $SiNH_2$, and OD where the DEA/OD/$SiNH_2$ monomer feed ratio was 100:50:50. As above, N435-catalyzed terpolymerizations were conducted at 70 °C, in bulk. However, under reaction condition A, no vacuum was applied until 40 h as described above. In contrast, the terpolymerization for condition B was performed by applying a vacuum at 1 h of 100 mmHg that was decreased stepwise to 25 and 2 mmHg by reaction times of 23 and 46 h, respectively. Regardless of whether reaction condition A or B was used, Figure 3 shows that formation of amide links (DEA−SiAA units) occur more rapidly than ester repeats (DEA−OA units). Furthermore, little difference in the rate of amide unit formation was observed under conditions A and B. For DEA−OA unit formation, the use of vacuum earlier in reactions for conditions B led to more rapid conversion to ester units. More rapid formation of amide units relative to ester units observed for terpolymerization in Table 4 and Figure 3 is in contrast to above (Figure 2 and Table 3), where ester formation was relatively more rapid. Conversion to DEA−SiAA units was higher than that of DEA−OA units throughout terpolycondensations. For example, after 1 h, the amine functional group consumption reached 88% whereas consumption of hydroxyl functionality under conditions A and B by 1 h reached 55 and 61%, respectively. For conditions A and B, amine functional group conversion slowly approached 98% by 70 h while hydroxyl consumption converged to similar values (∼ 90%) by 70 h (Figure 3). Inspection of Table 4 provides values of amide-to-ester units that correspond to the above functional group conversion values. This difference between relative reactivity observed by comparison of Figures 2 and 3 can be explained since the potential quantity of ester groups that can be formed for the terpolymerization decreased by a factor of 2 while total ethanol that can be formed as a byproduct remains unchanged. While ethanol formation for terpolymerizations has little effect on conversion to DEA−SiAA units, ethanol is a competitive nucleophile with hydroxyl terminal groups slowing the rate of DEA−OA unit formation. It is noteworthy that a control terpolymerization reaction, performed exactly as above (70 °C, bulk) under condition A, but without addition of N435, gave only a mixture of monomers and dimers (Table 4).

GPC chromatograms for terpolymerizations described in Table 4 performed using condition A are displayed in Figure 4. Values of M_n and PDI corresponding to these chromatograms are given in Table 4. Also, Figure 4 shows the GPC trace obtained from a nonpolymerized mixture of the monomers. By 1 h, GPC peaks corresponding to OD and DEA at 4.9 and 4.7 mL elution times are no longer observed, suggesting their rapid conversion to oligomers. By 70 h, the peak at 4.3 mL corresponding to $SiNH_2$ does not appear as a shoulder, indicating

Table 4. N435-Catalyzed Terpolymerizations (70 °C, in Bulk) between Diethyl Adipate, Octanediol, and PDMS-Diamine, Using a Monomer Feed of 100:50:50 with Reaction Conditions A and B

	polycondensation at reaction conditions A[a]					polycondensation at reaction conditions B[b]					control reaction[c]		
time (h)	Am/Es ratio[d]	P_n[e]	M_n NMR[f]	M_n[g]	PDI[g]	Am/Es ratio[d]	P_n[e]	M_n NMR[f]	M_n[g]	PDI[g]	P_n[e]	M_n[g]	PDI[g]
1	1.6:1	3.5	1130	680	2.4	1.5:1	4.1	1320	770	2.3	1.3	940	2.9
4	1.6:1	4.1	1320	1000	2.4	1.3:1	6.0	1910	1400	2.3	1.4	950	2.8
16	1.4:1	5.2	1660	1200	2.3	1.3:1	8.5	2680	2140	2.2	1.5	1070	2.8
42	1.2:1	13.1	4110	3740	2.3	1.1:1	16.2	5070	5040	1.9	1.5	955	3.0
70	1.1:1	18.6	5820	7500	1.9	1.1:1	19.6	6130	6720	1.8	1.4	700	3.1

[a] 40 h at ambient pressure, 30 h at reduced pressure (10 mmHg). [b] 1 h at 100 mmHg, 23 h at 25 mmHg, 46 h at 2 mmHg. [c] Without N-435 (noncatalyzed). [d] From NMR: the ratio of integration values of $\mathbf{CH_2}$OCO/$\mathbf{CH_2}$NHCO. [e] From NMR: integration values of $\mathbf{CH_2}$OCO + $\mathbf{CH_2}$NHCO/$\mathbf{CH_2}$OH + $\mathbf{CH_2}$$NH_2$ end group. [f] M_n(NMR) = P_n × [(molecular weight of the repeat unit)/(number of monomers units in the repeat unit)] + molecular weight of end group. [g] From GPC.

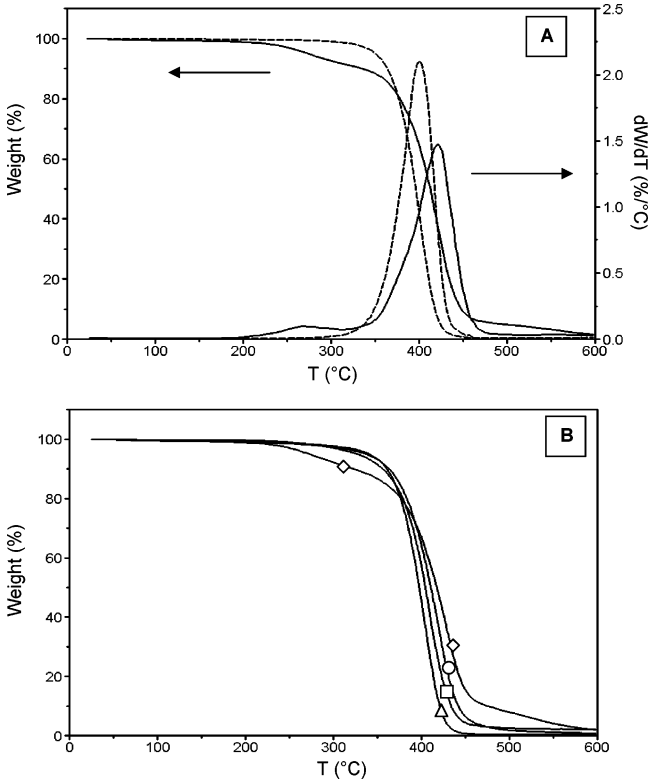

Figure 5. Thermogravimetric curves (10 °C/min, in N_2) of (A) homopolymers POA (broken line) and PSiAA (solid line) and (B) copolymers P(OA-*co*-80 mol % SiAA) (◇), P(OA-*co*-50 mol % SiAA) (○), P(OA-*co*-33 mol % SiAA)] (□), and P(OA-*co*-16 mol % SiAA) (Δ).

its complete conversion to the terpolymer (M_n 7500, M_w/M_n 1.90).

Ultimately, at the end of reactions (70 h) using conditions A and B, similar values of total functional group conversion (p), terpolymer degree of polymerization, and M_n were obtained (see Table 4). Corresponding values of amide-to-ester units as reactions progressed to 68−70 h using conditions A and B approached very close to each other (i.e., 1.1/1). However, given the different relative rates of amide and ester formation under conditions A and B, and assuming exchange reactions at amide bonds along terpolymers occur slowly or not at all, the two products formed will be different with respect to distribution of DEA−SiAA and DEA−OA units. Block lengths of DEA−SiAA units would be expected to be longer for terpolymerizations conducted under conditions A. However, terpolymers prepared under conditions A and B should both have a microstructure that is blocky since the formation of DEA−SiAA units occurs more rapidly than DEA−OA units. The copolymers analyzed below are those obtained under reaction conditions A and described in Table 2.

Solid-State Properties. Thermal stability of silicone polyesteramides and of reference POA and PSiAA homopolymers was investigated by TGA both under nitrogen and under air purge. The thermogravimetric curves (in N_2) are shown in Figure 5. In agreement with earlier results,[33] POA (Figure 5A, broken line) thermally degrades in a single step with a maximum rate of decomposition at 400 °C (T_{max}). Three thermal decomposition regions can be identified in the TGA curve of PSiAA (Figure 5A, solid line). The main step is located at T_{max} = 421 °C, i.e., at a temperature higher than T_{max} of POA, followed by a region of slow weight loss ranging from 450 to 600 °C. A clear weight loss step centered at 275 °C precedes the main degradation. Comparison of the TGA curve of PSiAA with literature data is difficult because, to our knowledge, no thermal degradation results are available for polydimethylsiloxane adipamides. On the contrary, thermal stability of linear polydimethylsiloxane (PDMS) has been widely studied. A recent paper[37] reports a two-step TGA curve in PDMS containing a fraction of low molecular weight chains. This behavior is attributed to molecular mass heterogeneity, since it is known that PDMS thermal stability is molecular weight dependent.[34−37] However, the molecular weight distribution of the present PSiAA is both rather narrow (Table 2) and unimodal. Hence, the peculiar multistep TGA curve of PSiAA (Figure 5A) is tentatively attributed to the presence along the polymer chain of adipic units and amide linkages.

Figure 5B shows selected TGA curves of copolyesteramides. The TGA curves of copolymers with A-unit content ≤16 mol % are identical to that of POA. Hence, only the P(OA-*co*-16 mol % SiAA) curve is shown in Figure 5B as an example. When the content of A-units exceeds 16 mol %, the main degradation step gradually shifts to higher temperature. The copolymer richest in A-units (80 mol %) shows an additional low-T weight loss, similar to that observed in Figure 5A for PSiAA, as well as a slow weight decrease above 450 °C, reminiscent of that of PSiAA. All investigated samples display a very similar solid residue at 600 °C, which ranges between 0.5% and 2%.

Thermogravimetric experiments were also performed under air purge (curves not shown). Analogous to the behavior under N_2 purge (Figure 5A), in air POA degrades at lower temperature than PSiAA (T_{max} = 377 °C for POA vs 419 °C for PSA). However, in air, the thermal stability difference between POA and PSiAA is larger than in nitrogen, owing to a marked decrease in POA degradation temperature under air purge. In air, the main thermal degradation of P(OA-*co*-SiAA) copolymers undergoes a gradual shift toward higher temperatures with increasing A-unit content, as was already observed in nitrogen (Figure 5B). The change from nitrogen to air atmosphere is found to strongly affect the solid residue of PSiAA at 600 °C, which increases from 1.6% to 18.3%. Analogous behavior is shown by silicone polyesteramide copolymers whose residue at 600 °C increases with A-unit content in air, unlike the quasi-constant value displayed under nitrogen. Similar to earlier work on PDMS,[37] the high-temperature solid residue observed when both PSiAA and silicone polyesteramide copolymers are analyzed in air is attributed to silica (SiO_2), produced by oxidation reactions involving dimethylsiloxane blocks.

In silicone copolyesteramides investigated in this work, comonomer composition (i.e., A:B molar ratio) is found to strongly affect physical characteristics of the materials, which changes from hard to sticky, with an intermediate composition range displaying a waxy appearance (Table 2). WAXS diffractograms were collected for both solid and waxy samples (A-unit content from 0 to 16 mol %) and are shown in Figure 6. X-ray diffractograms for all copolymers are similar to that of POA (curve a), with reflections located at the same positions. This result indicates that copolymers rich in B-units develop a POA-type crystal phase. The degree of crystallinity (χ_c) of analyzed copolymers, calculated from diffractograms as the ratio of crystalline peak areas to total area under the scattering curve, is listed in Table 5. Since the results of both WAXS and DSC depend on the mass of the analyzed samples, copolymer composition in Table 5 is expressed on a weight basis. The degree of crystallinity of the copolymers decreases with increasing A-unit content and is still appreciable in the waxy copolymer P(OA-*co*-16 mol % SiAA) that contains 43 wt % A-units.

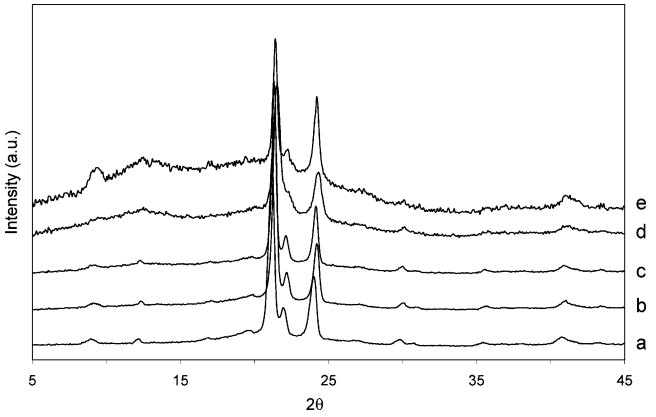

Figure 6. WAXS diffractograms of POA (a), P(OA-*co*-2 mol % SiAA) (b), P(OA-*co*-5 mol % SiAA) (c), P(OA-*co*-10 mol % SiAA) (d), and P(OA-*co*-16 mol % SiAA) (e).

Table 5. Melting and Crystallinity Data of POA and Copolyesteramides

sample	A:B weight ratio[a]	χ_c[b] (%)	ΔH_m[c] (J/g)	ΔH_m[d] (J/g)
POA	0:100	63	108	104
P(OA-*co*-2 mol % SiAA)	6:94	52	98	96
P(OA-*co*-5 mol % SiAA)	18:82	55	87	85
P(OA-*co*-10 mol % SiAA)	30:70	40	67	65
P(OA-*co*-16 mol % SiAA)	43:57	20	56	54
P(OA-*co*-33 mol % SiAA)	66:34		22	22
P(OA-*co*-50 mol % SiAA)	79:21		8	7
P(OA-*co*-80 mol % SiAA)	94:6		0	0

[a] Calculated taking into account the molecular weight of A- and B-units (Scheme 2) and the amide/ester ratio (Table 2). [b] From WAXS. [c] From DSC: heating scan after controlled cooling (at −10 °C/min). [d] From DSC: heating scan after quench cooling.

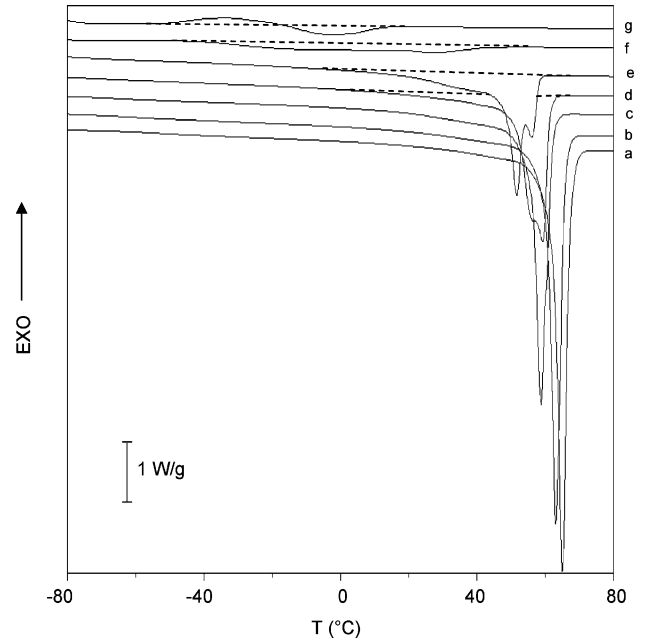

Figure 7. DSC heating scans (20 °C/min, after controlled cooling at 10 °C/min) of POA (a), P(OA-*co*-2 mol % SiAA) (b), P(OA-*co*-5 mol % SiAA) (c), P(OA-*co*-10 mol % SiAA) (d), P(OA-*co*-16 mol % SiAA) (e), P(OA-*co*-33 mol % SiAA) (f), and P(OA-*co*-50 mol % SiAA) (g). Broken lines are drawn as guidelines to highlight the endo- and exothermal phenomena.

DSC experiments were performed on all copolymers, including those with a sticky appearance. Figure 7 shows DSC curves after controlled cooling of POA and of selected copolymers over a temperature range where crystallization and melting phenomena appear. POA (curve a) is a partially crystalline polyester that melts at 67 °C, in agreement with earlier results.[33] The DSC curves of copolyesteramides show melting endotherms, whose temperature location and area decrease with increasing A-unit content. The decrease of melting enthalpy agrees with the decrease of crystallinity obtained by X-ray diffraction (Table 5). DSC curves in Figure 7 clearly show that it is the location of the melting process relative to room temperature (RT) that determines the physical appearance of copolymers. When melting occurs above RT, i.e., for P(OA-*co*-2 mol % SiAA) (curve b) and P(OA-*co*-5 mol % SiAA) (curve c), the material is a solid. In contrast, when the fusion process partially overlaps room temperature, i.e., for P(OA-*co*-10 mol % SiAA) (curve d) and P(OA-*co*-16 mol % SiAA) (curve e), the material is waxy at RT owing to melting of the least perfect crystals at or below RT.

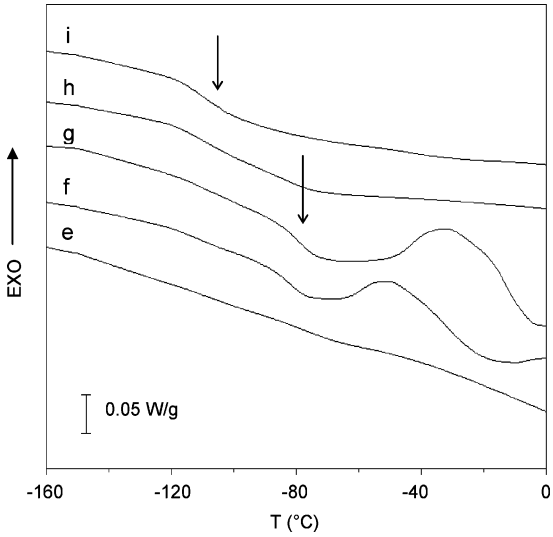

Figure 8. DSC heating scans (20 °C/min, after quench cooling from melt) of P(SiAA) (i), P(OA-*co*-80 mol % SiAA) (h), P(OA-*co*-50 mol % SiAA) (g), P(OA-*co*-33 mol % SiAA) (f), and P(OA-*co*-16 mol % SiAA) (e). Arrows indicate glass transitions.

Interestingly, Figure 7 shows that copolymers P(OA-*co*-33 mol % SiAA) and P(OA-*co*-50 mol % SiAA), which are sticky at RT, are able to generate a crystal phase whose stability range is below RT. The DSC curve of P(OA-*co*-33 mol % SiAA) (curve f) shows a very broad melting endotherm and no exothermal events, whereas sample P(OA-*co*-50 mol % SiAA) (curve g) exhibits cold crystallization and melting phenomena of identical magnitude ($\Delta H_c = \Delta H_m = 8$ J/g). In this copolymer the crystal phase forms and melts during the heating run. In the experimental conditions adopted (heating at 20 °C/min after controlled cooling at 10 °C/min), no crystal phase is observed in the copolymer with 80 mol % of A-units (curve not shown).

In order to investigate thermal transitions of the amorphous phase of P(OA-*co*-SiAA) copolymers, DSC heating scans were carried out on melt quenched samples. Figure 8 displays DSC curves of PSiAA and selected copolymers rich in A-units. Polyamide PSiAA (curve i) shows a glass transition (T_g) at −106 °C, higher than that reported in the literature for PDMS ($T_g = -123$ °C).[38] The copolymer containing 80 mol % A-units (curve h) exhibits a broad glass transition region that initially corresponds with the PSiAA glass transition but then spans about 40 °C. Both P(OA-*co*-50 mol % SiAA) and P(OA-*co*-33 mol % SiAA) show a clear glass transition around −80 °C that is followed by a cold crystallization exotherm (curves g and f, respectively). Melting of the cold crystallized phase in P(OA-*co*-50 mol % SiAA) involves an enthalpy

(Table 5) identical to that of cold crystallization ($\Delta H_c = 7$ J/g). In contrast, cold crystallizationand melting enthalpies for P(OA-*co*-33 mol % SiAA) differ ($\Delta H_c = 3$ J/g, $\Delta H_m = 22$ J/g), showing that crystallinity partially develops in this sample during the melt quenching process. The existence of such crystals, which act as heterogeneous nucleants, explains the observed early start of cold crystallization in this copolymer compared with that of P(OA-*co*-50 mol % SiAA), in spite of their identical T_g's. Close examination of all DSC curves in Figure 8 suggests that two glass transitions coexist in these copolyesteramides (arrows in Figure 8): one at lower T associated with siliconamide segments and the other, above which POA crystallization may occur, attributed to mobilization of POA sequences. The presence of a crystal phase in most of the analyzed copolymers (see ΔH_m in Table 5) does not allow comparison of intensities for the two glass transition phenomena. It would be anticipated that, for amorphous samples, intensities for these glass transitions would change with composition. When a consistent POA crystal phase is present, such as in sample P(OA-*co*-16 mol % SiAA), no clear glass transition is detected (curve e).

Thermal characterization results show that, except for copolymer P(OA-*co*-80 mol % SiAA) which contains only 6 wt % octamethylene adipate B-units, all copolyesteramides investigated in this work are able to develop a POA crystal phase. This result is consistent with the well-known crystallizability of linear aliphatic polyesters, enhanced by the high flexibility of polysiloxane segments.

Conclusions

The synthesis of polyesteramides containing siloxane units was performed successfully by lipase catalysis at 70 °C in bulk. In addition, the syntheses of POA and PSiAA were performed using the same reaction conditions. ^{1}H NMR analysis revealed that synthesized copolymers consist of amide (DEA−SiAA) and ester (DEA−OA) repeat units. The ratios of amide/ester links in copolymers agrees with the monomer feed ratio. Except for P(OA-*co*-33 mol % SiAA), PSiAA and all other copolyesteramide compositions had M_n and PDI values that ranged from 6 to 11 kDa and 1.5−2.2, respectively. Formation of amide links (DEA−SiAA units) occurs more rapidly than ester repeats (DEA−OA units). This results in copolymers that tend toward a blocklike sequence distribution. The DEA/OD/Si-NH_2 monomer feed ratio, and, consequently, the ratio between amide and ester units along the chain, strongly affects the physical aspect of copolymers. Synthesized silicone-containing copolyesteramides changed from hard solid materials when rich in octamethylene adipate units with well-developed high melting crystal phases to sticky glues when α,ω-(diaminopropyl)polydimethylsiloxane adipamide is the major component. Two constant-T glass transitions are revealed by DSC, attributed to siliconamide and POA sequences. A POA crystal phase develops in all P(OA-*co*-SiAA) copolymers with at least 50 mol % (21 wt %) POA units. As expected, the melting of POA crystals occurs at temperatures that decrease with increasing foreign siliconamide units along the copolymer chain.

Acknowledgment. We thank the National Science Foundation Industrial/University Cooperative Research Center for Biocatalysis and Bioprocessing of Macromolecules at the Polytechnic University and the Italian Ministry for University and Research (MUR) for their financial support of this work.

References and Notes

(1) Grigoras, S.; Lane, T. H. *Conformation Analysis of Substituted Polysiloxanes Polymers, In Silicon-Based Polymer Science: A Comprehensive Resource*; Zeigler, J. M., Fearon, F. W. G., Eds.; Adv. Chem. Ser. 224; American Chemical Society: Washington, DC, 1990; Chapter 7, p 125.
(2) Brook, M. A. *Silicon in Organic, Organometallic and Polymer Chemistry*; John Wiley and Sons: New York, 2000; Chapter 2.
(3) Noll, W. *Chemistry and Technology of Silicones*; Academic Press: New York, 1968; pp 439−440.
(4) Stepto, R. F. T. Theoretical Aspects of Conformation-Dependent Properties. In *Siloxane Polymers*; Clarson, S. J., Semlyen, J. A., Eds.; Prentice Hall: Englewood Cliffs, NJ, 1993; Chapter 8, p 373.
(5) Tomanek, A. *Silicones and Industry*; Hanser (Wacker Chemie): Munich, 1991.
(6) Owen, M. J. Surface Chemistry and Applications. In *Siloxane Polymers*; Clarson, S. J., Semlyen, J. A., Eds.; Prentica Hall: Englewood Cliffs, NJ, 1993; Chapter 7, p 309.
(7) Tang, L.; Sheu, M. S.; Chu, T.; Huang, Y. H. *Biomaterials* **1999**, *20*, 1365−1370.
(8) Haupt, M.; Knaus, S.; Rohr, T.; Grubber. H. *J. Macromol. Sci., Pure Appl. Chem.* **2000**, *A37*, 323−341.
(9) Wulff, G.; Schmid, J.; Venhoff, T. *Macromol. Chem. Phys.* **1996**, *197*, 259−274.
(10) Myiata, T.; Nakamae, K. *Trends Polym. Sci.* **1997**, *5*, 198−206.
(11) Toki, T.; Harada, M.; Inaba, Y. US Patent 5,504,185, 1996.
(12) Speck, S. B. *J. Org. Chem.* **1953**, *18*, 1689−1700.
(13) Kovacs, H. N.; Delman, A. D.; Simms, B. B. *J. Polym. Sci., Polym. Chem.* **1968**, *6*, 2103−2115.
(14) Sacripante, G. G.; Macaneny, B. T. US Patent 5,401,601, 1995.
(15) Yilgor, E.; Yilgor, I.; Suzer, S. *Polymer* **2003**, *44*, 7271−7279.
(16) Yilgor, I.; Steckle, W. P. J.; Yilgor, E.; Freelin, R. G.; Riffle, J. S. *J. Polym. Sci., Polym. Chem.* **1989**, *27*, 3673−3690.
(17) Hood, J. D.; Blount, W. W.; Sade, W. T. *J. Coat. Technol.* **1986**, *58*, 49−52.
(18) Ghatge, N. D.; Jadhav, J. Y. *J. Polym. Sci., Polym. Chem. Ed.* **1984**, *22*, 1565−1572.
(19) Yang, J.; Zhou, S.; You, B.; Wu, L. Preparation and surface properties of silicone-modified polyester-based polyurethane coats. *JCT Res.* 3.4 (Oct 2006): 333(7)].
(20) Liu, H. J.; Lin, L. H.; Chen, K. M. *Text. Res. J.* **2003**, *73*, 583−587.
(21) Stevens, M. P. *Polymer Chemistry: An Introduction*, 3rd ed.; Oxford University Press: New York, 1999.
(22) Henkensmeier, D.; Abele, B. C.; Candussio, A.; Thiem, J. *Polymer* **2004**, *45*, 7053−7059.
(23) Uyama, H.; Kobayashi, S. *Adv. Polym. Sci.* **2006** *194*, 133−158.
(24) Hu, J.; Gao, W.; Kulshrestha, A. S.; Gross, R. A. *Macromolecules* **2006**, *39*, 6789−6792.
(25) Hunsen, M.; Azim, A.; Mang, H.; Wallner, S. R.; Ronkvist, A.; Xie, W.; Gross, R. A. *Macromolecules* **2007**, *40*, 148−150.
(26) (a) Tanaka, A; Kawamoto, T.; Sonomoto, K. *Ann. N.Y. Acad. Sci.* **1990**, *613*, 702−706. (b) Kawamoto, T.; Sonomoto, K;, Tanaka, A. *J. Biotechnol.* **1991**, *18*, 85−91.
(27) Uejima, A.; Fukui, T.; Fukusaki, E.; Omata, T.; Kawamoto, T.; Sonomoto, K.; Tanaka, A. *Appl. Microbiol. Biotechnol.* **1993**, *38*, 482−486.
(28) Sahoo, B.; Brandstadt, K. F.; Lane, T. H.; Gross, R. A. *Org. Lett.* **2005**, *7*, 3857−3860.
(29) Rantwijk, F. Van; Hacking, M. A. P. J.; Sheldon, R. A. *Monatsh. Chem.* **2000**, *131*, 549−569.
(30) Zoete, M. C. de; Dalen, A. C. K.; Rantwijk, F. van; Sheldon, R. A. *J. Mol. Catal. B: Enzym.* **1996**, *2*, 141−145.
(31) Brandstadt, K. F.; Lane, T. H.; Gross, R. A. 20040082024, April 29, 2004.
(32) Kulshrestha, A. S.; Gao, W.; Gross, R. A. *Macromolecules* **2005**, *38*, 3193−3204.
(33) Fu, H.; Kulshrestha, A. S.; Gao, W.; Gross, R. A.; Baiardo, M.; Scandola, M. *Macromolecules* **2003**, *36*, 9804.
(34) Clarson, S. J.; Semiyen, J. A. *Polymer* **1986**, *27*, 91.
(35) Grassie, N.; MacFarlane, I. G. *Eur. Polym. J.* **1978**, *14*, 875.
(36) Lewis, C. W. *J. Polym. Sci.* **1959**, *32*, 425.
(37) Tiwari, A.; Nema, A. K.; Das, C. K.; Nema, S. K. *Thermochim. Acta* **2004**, *417*, 133.
(38) Brandrup, J.; Immergut, E. H.; Grulke, E. A. *Polymer Handobook*; John Wiley & Sons: New York, 1999.

MA070671I